Structural Studies of the O^{6}meG·C Interaction in the d(C-G-C-G-A-A-T-T-C-O^{6}meG-C-G) Duplex†

Dinshaw J. Patel* and Lawrence Shapiro
Department of Biochemistry and Molecular Biophysics, College of Physicians and Surgeons, Columbia University, New York, New York 10032
Sharon A. Kozlowski
Polymer Chemistry Department, AT&T Bell Laboratories, Murray Hill, New Jersey 07994
Barbara L. Gaffney and Roger A. Jones
Department of Chemistry, Rutgers, The State University of New Jersey, New Brunswick, New Jersey 08903
Received July 16, 1985

ABSTRACT: One- and two-dimensional nuclear magnetic resonance (NMR) experiments have been undertaken to investigate the conformation of the d(C_1-G_2-C_3-G_4-A_5-A_6-T_7-T_8-C_9-O^{6}meG$_{10}$-C_{11}-G_{12}) self-complementary dodecanucleotide (henceforth called O^{6}meG·C 12-mer), which contains C3·O^{6}meG10 interactions in the interior of the helix. We observe intact base pairs at G2·C11 and G4·C9 on either side of the modification site at low temperature though these base pairs are kinetically destabilized in the O^{6}meG·C 12-mer duplex compared to the G·C 12-mer duplex. One-dimensional nuclear Overhauser effects (NOEs) on the exchangeable imino protons demonstrate that the C3 and O^{6}meG10 bases are stacked into the helix and act as spacers between the flanking G2·C11 and G4·C9 base pairs. The nonexchangeable base and H1′, H2′, H2″, H3′, and H4′ protons have been completely assigned in the O^{6}meG·C 12-mer duplex at 25 °C by two-dimensional correlated (COSY) and nuclear Overhauser effect (NOESY) experiments. The observed NOEs and their directionality demonstrate that the O^{6}meG·C 12-mer is a right-handed helix in which the O^{6}meG10 and C3 bases maintain their anti conformation about the glycosidic bond at the modification site. The NOEs between the H8 of O^{6}meG10 and the sugar protons of O^{6}meG10 and adjacent C9 exhibit an altered pattern indicative of a small conformational change from a regular duplex in the C9–O^{6}meG10 step of the O^{6}meG·C 12-mer duplex. We propose a pairing scheme for the C3·O^{6}meG10 interaction at the modification site. Three phosphorus resonances are shifted to low field of the normal spectral dispersion in the O^{6}meG·C 12-mer phosphorus spectrum at low temperature, indicative of an altered phosphodiester backbone at the modification site. These NMR results are compared with the corresponding parameters in the G·C 12-mer, which contains Watson–Crick base pairs at the same position in the helix.

Nuclear magnetic resonance is a powerful method for monitoring the conformation and dynamics of DNA helices at the individual base pair level in aqueous solution (Patel et al., 1982a; Kearns, 1984). This technique is especially powerful at probing modified sites in DNA such as base pair mismatches and helix interruptions and providing both structural and hydrogen-exchange information both at and adjacent to the modification site (Patel et al., 1982b). We extend these investigations below to covalent modifications of DNA and have undertaken a systematic study of the structural effects of O^6-alkylation of guanosine in the interior of DNA helices.

Alkylation of DNA is the simplest of modifications and methylation at the O^6 position of guanosine (O^{6}meG) has profound biological implications. Thus, O^{6}meG formation in DNA resulting from exposure to diazoalkanes and nitrosamines is a carcinogenic event (Loveless, 1969; Singer, 1979; Cairns, 1981; Singer & Grunberger, 1983).

The consequences of O^{6}meG modification are best investigated if spectroscopic studies can be undertaken on short oligonucleotides containing a single modification site. The synthesis methodology has been worked out, and O^{6}meG-containing tetranucleotides (Fowler et al., 1982), hexanucleotides (Kuzmich et al., 1983), and dodecanucleotides (Gaffney et al., 1984) have been synthesized recently. The O^{6}meG-containing tetranucleotide has been incorporated into viral and plasmid genomes (Green et al., 1984) to study in vivo mutagenesis at a unique site in a viral genome (Loechler et al., 1984).

The recent synthesis and characterization of the four self-complementary dodecanucleotides d(C-G-N-G-A-A-T-T-C-O^{6}meG-C-G), where N = C, T, A, and G (Gaffney et al., 1984), are of considerable interest. These workers demonstrated that incorporation of O^{6}meG·N interactions at position 3 from either end of the duplex results in a 19–26 °C destabilization of the helix–coil transition. We have undertaken a systematic one- and two-dimensional NMR investigation of all four modified dodecanucleotides and report in this paper on the O^{6}meG·C analogue and in the following paper (Patel et al., 1986) on the O^{6}meG·T analogue. We have already reported on the parent sequence containing standard G·C pairs (Patel et al., 1982c; Hare et al., 1983) so that the consequences of O^{6}meG incorporation can be evaluated in structural terms in aqueous solution.

Experimental Procedures

The d(C-G-C-G-A-A-T-T-C-O^{6}meG-C-G) dodecanucleotide synthesis, purification, and analysis have been reported previously (Gaffney et al., 1984). The sample was >97% pure as judged from its proton NMR spectrum in H_2O and D_2O solution. The O^{6}meG·C 12-mer was dissolved to a concen-

† This research was supported by National Institutes of Health Grant 1R01 GM34504 to D.J.P. and by American Cancer Society Grant CH-248 and National Institutes of Health Grant GM 31483 to R.A.J. L.S. was supported by Biochemical Research Support Grant SO7RR05359-23.

0006-2960/86/0425-1027$01.50/0

Chart I

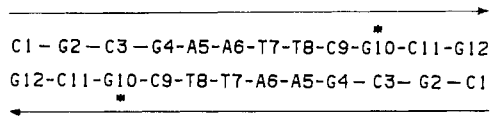

tration of 200 A_{260} units in 0.4 mL in 0.1 M NaCl, 10 mM phosphate, and 1 mM ethylenediaminetetraacetic acid (EDTA) buffer for recording of NMR spectra.

One-dimensional proton NMR spectra of the O^{6}meG·C 12-mer in H_2O were recorded on a JEOL GX-500 using a timed-shared Redfield long pulse to null the solvent water signal (Redfield et al., 1975; Haasnoot & Hilbers, 1983). The nuclear Overhauser measurements using a set of decoupling frequencies were accumulated in the interleave mode. The experimental conditions are included in the figure captions. Phosphorus spectra were accumulated on a Varian XL-200 spectrometer. Chemical shifts are corrected for the temperature dependence of the internal standard trimethyl phosphate.

Two-dimensional proton correlated (COSY) and nuclear Overhauser effect (NOESY) data sets (Feigon et al., 1983; Hare et al., 1983; Scheek et al., 1984; Weiss et al., 1984) were recorded with quadrature detection for the O^{6}meG·C 12-mer in D_2O solution on the Yale WM-500 spectrometer. We collected 512 t_1 increments over a sweep range of 4400 Hz, using 1024 complex points in the t_2 dimension. The data sets were transferred to magnetic tape and processed on the Columbia VAX 11-780 using the Hare two-dimensional processing software. The magnitude COSY data were collected with a repetition delay of 1.5 s. They were apodized in t_2 and t_1 with an unshifted sine bell function that was zeroed at the 600th point and Fourier-transformed in both dimensions. The phase-sensitive NOESY data (States et al., 1982) were collected for a 250-ms mixing time with a repetition delay of 1.5 s. The data sets were Fourier-transformed in both dimensions without application of window functions. Symmetrized contour plots were recorded on a 22-in. Zeta 822 plotter for analysis and assignment of resonances and on a HP 7475A plotter for publication figures, both of which were interfaced to a VAX 11-780.

Results

The bases in the self-complementary d(C_1-G_2-C_3-G_4-A_5-A_6-T_7-T_8-C_9-O^{6}meG$_{10}$-C_{11}-G_{12}) duplex are numbered 1–12 (Chart I). We designate this modified dodecanucleotide as O^{6}meG·C 12-mer in the rest of this paper.

Exchangeable Imino and Amino Protons. The 500-MHz proton NMR spectrum of the O^{6}meG·C 12-mer duplex in 0.1 M NaCl, 10 mM phosphate, and H_2O, pH 7.02 at 10 °C between 6 and 15 ppm is presented in Figure 1A. The imino protons resonate between 12 and 14 ppm while the amino and nonexchangeable base protons resonate between 6 and 8.5 ppm. The imino protons in the O^{6}meG·C 12-mer duplex have been assigned from one-dimensional NOE measurements recorded at −5 and 10 °C with the difference spectra at the latter temperature recorded in Figure 1B–D.

We can differentiate between the imino protons of T7 and T8 at lowest field since saturation of the 13.85 ppm imino proton exhibits an NOE at the adjacent 12.36 ppm guanosine imino proton (data not shown) while this effect is absent on saturation of the 13.73 ppm imino proton (Figure 1B) in the O^{6}meG·C 12-mer duplex at 10 °C. We can therefore assign the 13.73, 13.85, and 12.36 ppm resonances to the imino protons of base pairs A6·T7, A5·T8, and G4·C9, respectively (Table I). The adenosine H2 protons can be assigned from intra and inter base pair NOEs from the known thymidine imino proton assignments, and these are listed in Table I.

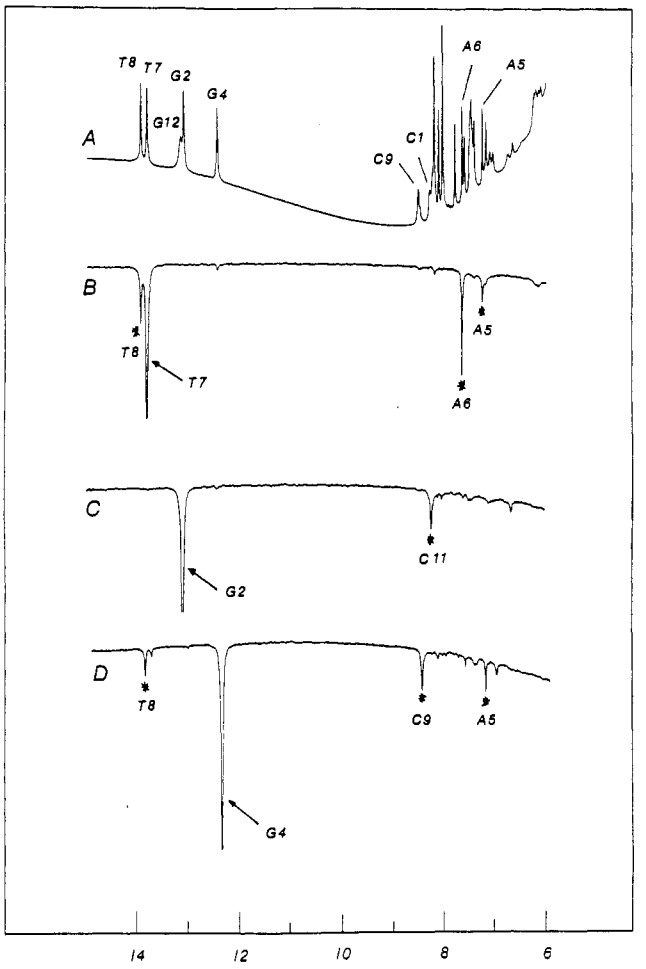

FIGURE 1: (A) 500-MHz proton NMR spectrum (6–15 ppm) of the O^{6}meG·C 12-mer in 0.1 M NaCl, 10 mM phosphate, and 1 mM EDTA in H_2O, pH 7.02 at 10 °C. Difference spectra following 1-s saturation of (B) the 13.73 ppm thymidine imino proton, (C) the 13.01 guanosine imino proton, and (D) the 12.36 guanosine imino proton. Saturation power levels resulted in ~50% saturation of the desired resonance. The saturated resonance is designated by an arrow while the observed NOEs are designated by asterisks.

Table I: Proton Chemical Shifts of the Thymidine Imino, Guanosine Imino, Cytidine Amino, and Adenosine H2 Protons in the O^{6}meG·C 12-mer at 10 °C[a]

pair	T H3	G H1	C H4[b]	A H2
C1·G12		13.07	8.20	
G2·C11		13.01	8.14	
C3·O^{6}meG10				
G4·C9		12.36	8.41	
A5·T8	13.85			7.16
A6·T7	13.73			7.57

[a] Buffer is 0.1 M NaCl, 10 mM phosphate, 1 mM EDTA, and H_2O, pH 7.02. [b] Chemical shift represents hydrogen-bonded cytidine amino proton.

Saturation of the 12.36 ppm imino proton of G4·C9 exhibits an NOE in one direction only to the 13.85 ppm imino proton of adjacent A5·T8 for the O^{6}meG·C 12-mer duplex at 10 °C (Figure 1D). The C3·O^{6}meG10 interaction lacks an imino proton and can act as a spacer between the G4·C9 and G2·C11 base pairs. There are two remaining imino protons at 13.07 and 13.01 ppm in the spectrum of the O^{6}meG·C 12-mer at 10 °C (Figure 1A). The former imino proton is broad due to fraying at the ends of the helix (Patel & Hilbers, 1975) and is assigned to the C1·G12 base pair while the latter is assigned to the G2·C11 base pair. We do not observe an NOE at the

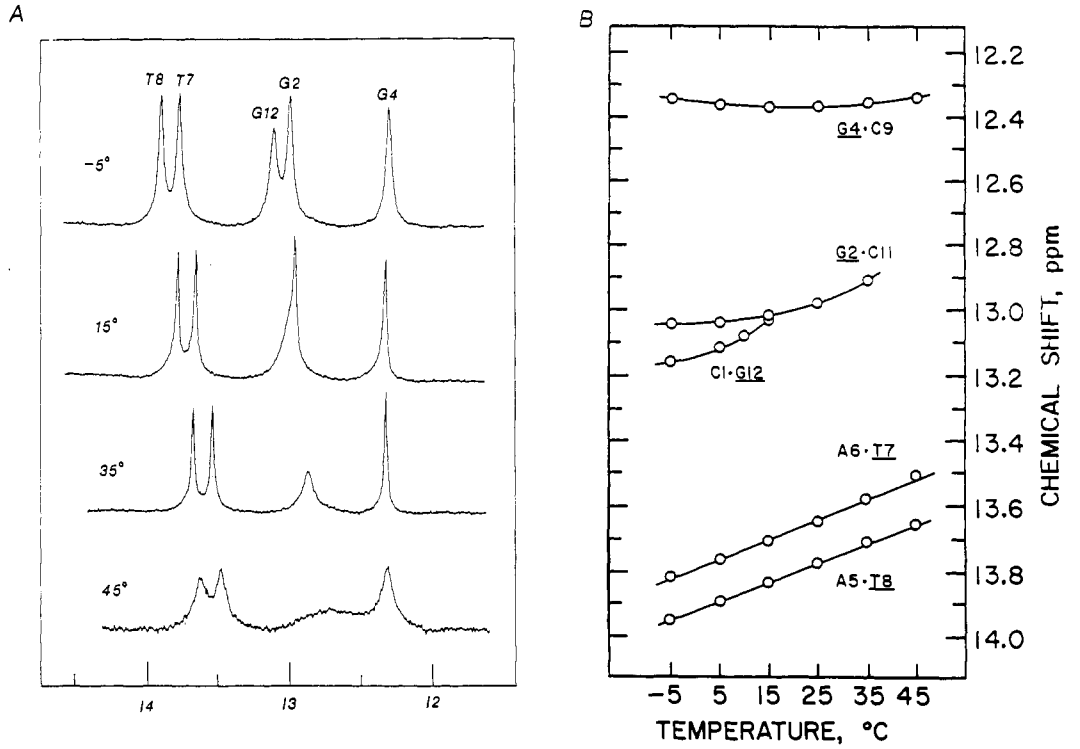

FIGURE 2: (A) 500-MHz proton NMR spectra (12–14 ppm) and (B) the temperature dependence of the chemical shifts of the O⁶meG·C 12-mer in 0.1 M NaCl, 10 mM phosphate, and 1 mM EDTA in H_2O, pH 7.02, as a function of temperature between −5 and 45 °C. The imino proton assignments are designated over the resonances.

12.36 ppm imino proton of the G4·C9 base pair on saturation of the 13.01 ppm imino proton of the G2·C11 base pair in the O⁶meG·C 12-mer at 10 °C (Figure 1C). Thus, the C3·O⁶meG10 interaction once again acts as a spacer between the G2·C11 and G4·C9 base pairs in the modified dodecanucleotide duplex. We detect intramolecular NOEs at the hydrogen-bonded cytidine amino protons between 8.1 and 8.4 ppm on saturation of the guanosine imino protons (Patel, 1976; McConnel, 1984; Fazakerley et al., 1984) (Figure 1C,D), and the amino proton chemical shifts are also listed in Table I.

This completes the assignment of the hydrogen-bonded thymidine imino, guanosine imino, and cytidine amino exchangeable protons and the adenosine H2 nonexchangeable protons in the O⁶meG·C 12-mer at 10 °C (Table I).

We detect five resolved imino protons for the O⁶meG·C 12-mer in 0.1 M NaCl, 10 mM phosphate, and H_2O, pH 7.02 at −5 °C (Figure 2A). We observe sequential broadening of the imino protons at the ends of the helix on raising the temperature. Thus, the imino proton of C1·G12 broadens significantly by 20 °C while that of G2·C11 broadens out by 45 °C (Figure 2A). The imino protons of C4·G9, A5·T8, and A6·T7 broaden simultaneously above 45 °C with the onset of the melting transition of the O⁶meG·C 12-mer in 0.1 M NaCl solution.

The temperature dependence of the imino proton chemical shifts in the O⁶meG·C 12-mer in 0.1 M NaCl between −5 and 45 °C is plotted in Figure 2B. The imino protons of the A5·T8 and A6·T7 base pairs shift significantly upfield with increasing temperature while the imino proton of the G4·C9 base pair exhibits a temperature-independent chemical shift in this temperature range (Figure 2B). The temperature-dependent upfield shifts are also observed at the imino protons of C1·G12 and G2·C11 with the effect more pronounced at the terminal base pair in the O⁶meG·C 12-mer duplex.

Two-Dimensional Spectra in D_2O Solution. The 500-MHz proton NMR spectrum of the O⁶meG·C 12-mer in 0.1 M NaCl, 10 mM phosphate, and D_2O at 25 °C exhibits well-resolved resonances, which can be classified by type into the spectral ranges 7.0–8.2 ppm (pyrimidine base H6 and purine base H8 and H2), 5.2–6.2 ppm (sugar H1′ and pyrimidine base H5), 4.6–5.1 ppm (sugar H3′), 3.6–4.5 ppm (sugar H4′, H5′ and H5″), 1.8–3.0 ppm (sugar H2′ and H2″), and 1.2–1.5 ppm (thymidine CH_3). In addition, the O⁶-methyl of G10 resonates at 3.44 ppm in the O⁶meG·C 12-mer duplex at 25 °C.

We have recorded two-dimensional spectra of the O⁶meG·C 12-mer in 0.1 M NaCl and 10 mM phosphate at 25 °C with a contour plot of a magnitude COSY presented in Figure 3A and a phase-sensitive NOESY with a 250-ms mixing time shown in Figure 3B. The details of data processing conditions are outlined under Experimental Procedures.

The resolved cross peaks in the COSY spectrum (Figure 3A) reflect two-bond (H2′–H2″), three-bond (H1′–H2′, H2′–H3′, H3′–H4′, and base H5–H6), and four-bond (thymidine H6–CH_3) coupling constants. The resolved cross peaks in the 250-ms mixing time NOESY spectrum (Figure 3B) correspond to NOE effects between proton pairs separated by <4.5 Å. We analyze below individual regions of the NOESY (Figure 3B) and COSY (Figure 3A) contour plots, which yield the detailed spectral assignments of the O⁶meG·C 12-mer duplex at 25 °C.

Base to H1′ NOESY Correlations. The cross peaks between the base (7.0–8.2 ppm) and the sugar H1′ and cytidine H5 protons (5.2–6.2 ppm) are presented in an expanded NOESY contour plot of the O⁶meG·C 12-mer at 25 °C in Figure 4. It can be shown that the purine H8 and pyrimidine H6 will be <4.5 Å from their own sugar H1′ and the sugar H1′ in the 5′ direction but >4.5 Å from the sugar H1′ in the 3′ direction for a regular right-handed duplex. Thus, each of these base protons will exhibit an NOE to its own and 5′-flanking sugar proton (Feigon et al., 1983; Hare et al., 1983; Scheek et al., 1984; Weiss et al., 1984a) except C1, the terminal nucleotide that lacks a 5′-flanking sugar.

These connectivities between the base proton and its own

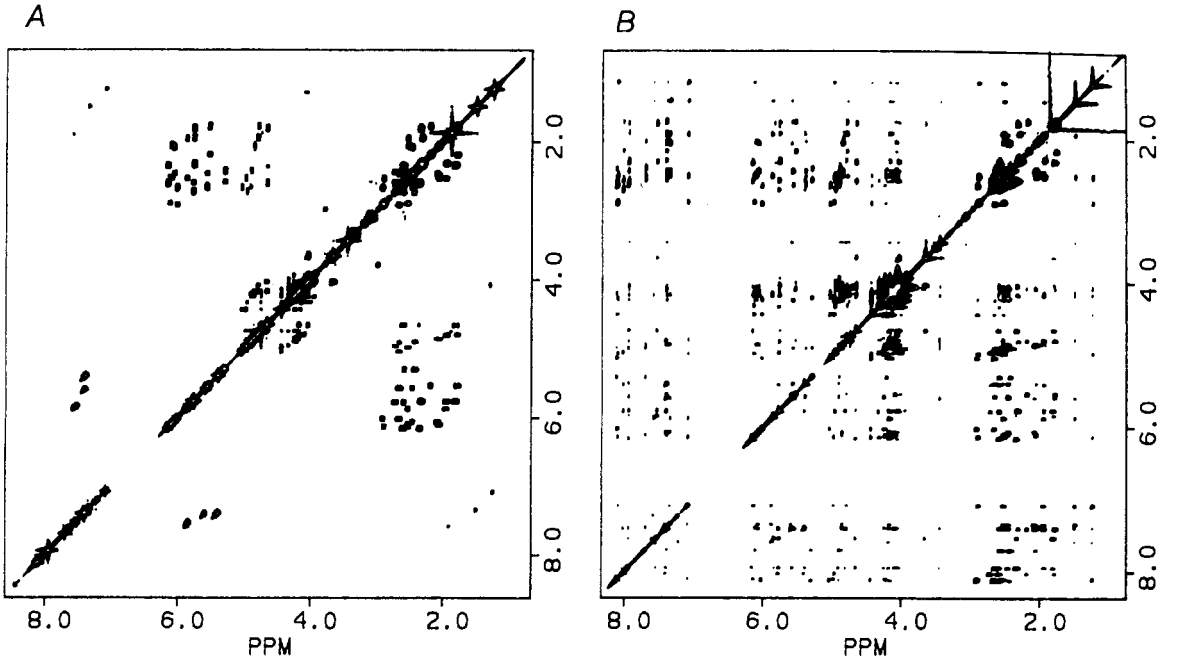

FIGURE 3: Contour plot of (A) the magnitude COSY spectrum and (B) the phase-sensitive NOESY spectrum (mixing time 250 ms) of the O^{6}meG·C 12-mer in 0.1 M NaCl, 10 mM phosphate, 1 mM EDTA, and D_2O at 25 °C.

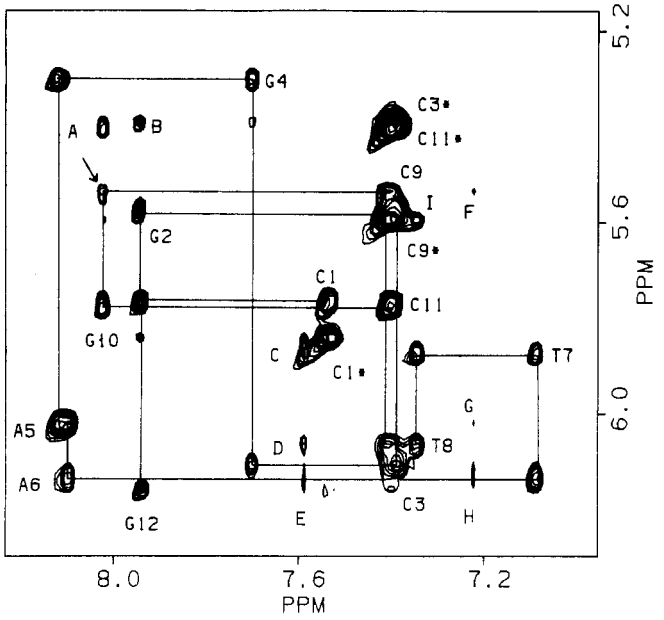

FIGURE 4: Expanded contour plot of the phase-sensitive NOESY spectrum (mixing time 250 ms) of the O^{6}meG·C 12-mer at 25 °C, establishing distance connectivities between the base protons (7.0–8.2 ppm) and the sugar H1′ protons (5.2–6.2 ppm). The base and sugar H1′ assignments are depicted next to the contour peaks while additional cross peaks designated by A–H are discussed and assigned in the text. The asterisks designate the cytidine H6 to H5 connectivities. The lines follow the connectivities between adjacent base protons through their intervening sugar H1′ protons.

and 5′-flanking sugar H1′ protons in the O^{6}meG·C 12-mer are drawn in Figure 4. The tracing is reasonably straightforward except for the O^{6}meG10–C11 segment, where the chemical shifts of the H1′ protons of these residues are similar. The base and sugar H1′ proton chemical shifts in the O^{6}meG·C 12-mer at 25 °C are listed in Table II.

We observe cross peaks of comparable intensities for the NOEs between the base proton and its own sugar H1′ and 5′-flanking sugar H1′ protons for the majority of the residues in the O^{6}meG·C 12-mer duplex 250-ms mixing time NOESY spectrum in Figure 4. We do note, however, that the cross peak between the H8 of O^{6}meG10 and the H1′ of C9 (designated by an arrow in Figure 4) is much weaker than the cross peak between the H8 and H1′ protons of O^{6}meG10, indicative of a conformational change in the vicinity of the alkylation site.

We also detect NOEs between the H2 proton of A6 and its own sugar H1′ proton (peak E, Figure 4), the sugar H1′ of T7 in the 3′ direction on the same strand (peak C, Figure 4), and the sugar H1′ of T8 in the opposite direction on the partner strand (peak D, Figure 4). Similarly, the H2 proton of A5 exhibits an NOE to its own H1′ (peak G, Figure 4), to the sugar H1′ of A6 in the 3′ direction on the same strand (peak H, Figure 4), and to the sugar H1′ of C9 in the opposite direction on the partner strand (peak F, Figure 4). These NOEs between the adenosine H2 proton and sugar H1′ protons exhibit directionality and are characteristic markers for a right-handed helix (Weiss et al., 1984b).

The cytidine H5 and thymidine CH_3 protons exhibit NOEs to the H1′ protons of their 5′-flanking sugars and not their own or 3′-flanking sugars in the O^{6}meG·C 12-mer duplex. We note, however, that the intensity of the cross peaks decreases in the order H5 of C3 to H1′ of G2 greater than H5 of C11 to H1′ of O^{6}meG10, which in turn is greater than H5 of C9 to H1′ of T8. We also observe NOEs between the CH_3 of T7 and the H1′ of A6 and the CH_3 of T8 and the H1′ of T7. These NOEs are characteristic of right-handed helices with the variations in cross-peak intensities reflecting conformational perturbations at the C3·O^{6}meG10 modification site in the O^{6}meG·C 12-mer duplex.

NOESY Correlations between Base Protons. The relative magnitudes of the NOEs between adjacent base protons (purine H8, pyrimidine H6, H5, and CH_3) are useful markers of DNA handedness. The expanded NOESY contour region covering the symmetrical spectral range 7.0–8.2 ppm of the O^{6}meG·C 12-mer is shown in Figure 5A. We observe NOEs between the purine H8 and pyrimidine H6 protons in the purine(3′–5′)pyrimidine G2–C3 step (peak B, Figure 5A), A6–T7 step (peak F, Figure 5A), and O^{6}meG10–C11 step (peak A, Figure 5A) on the same strand. Similarly, we detect NOEs between the purine H8 protons and pyrimidine H5 and

Table II: Base and Sugar Proton Chemical Shifts in the d(C-G-C-G-A-A-T-T-C-O^{6}meG-C-G) Duplex in 0.1 M NaCl, 10 mM Phosphate, and D_2O at 25 °C

	base				sugar				
	H8	H2	H6	H5/CH_3	H1′	H2′	H2″	H3′	H4′
C1			7.53	5.83	5.75	1.80	2.34	4.66	4.05
G2	7.93				5.55	2.66	2.45	4.90	4.24
C3			7.38	5.39	6.10	2.07	2.53	4.85	4.24
G4	7.68				5.29	2.45	2.60	4.90	4.20
A5	8.10	7.21			6.01	2.66	2.91	5.03	4.43
A6	8.08	7.58			6.15	2.53	2.91	4.96	4.43
T7			7.07	1.24	5.86	1.95	2.53	4.79	4.17
T8			7.33	1.50	6.05	2.07	2.45	4.85	4.17
C9			7.38	5.58	5.52	1.80	2.19	4.79	4.07
O^{6}meG10	8.01				5.77	2.72	2.60	4.96	4.32
C11			7.38	5.39	5.75	1.95	2.34	4.79	4.17
G12	7.93				6.15	2.60	2.34	4.66	4.17

CH_3 protons in the purine(3′–5′)pyrimidine G2–C3 step (peak B, Figure 4), A6–T7 step (peak G, Figure 5B), and O^{6}meG10–C11 step (peak A, Figure 4) on the same strand. By contrast, we do not detect NOEs between the purine H8 and pyrimidine H6, H5, and CH_3 protons in the pyrimidine-(3′–5′)purine steps on the same strand in the O^{6}meG·C 12-mer duplex. This directionality to the NOEs amongst base protons is characteristic of a right-handed duplex.

The NOEs between the H6 and H5 and CH_3 protons of adjacent pyrimidines are also characteristic of the handedness of the helix. Thus, we observe a strong NOE between the H6 of T7 and the CH_3 of T8 (peak H, Figure 5B) in the O^{6}meG·C 12-mer duplex. Similarly, the NOE between the H6 of T8 and the H5 of C9 (peak I, Figure 4) is stronger than that between the H6 of C9 and CH_3 of T8 (peak J, Figure 5B) in the modified dodecanucleotide duplex. This directionality is characteristic of right-handed duplexes.

Finally, NOEs are detected between the H2 protons of adjacent adenosines in the A5–A6 step (peak D, Figure 5A), the H6 protons of adjacent thymidines in the T7–T8 step (peak E, Figure 5A), and the H5 and CH_3 of adjacent pyrimidines in the T8–C9 step in the O^{6}meG·C 12-mer. Thus, we can monitor the A_5-A_6-T_7-T_8-C_9 segment through adjacent base–base NOEs without recourse to the sugar proton resonances.

H1′ to H2′ and H2″ COSY Connectivities. The cross section of the magnitude COSY spectrum of the O^{6}meG·C 12-mer between the sugar H1′ protons (5.2–6.3 ppm) and the sugar H2′ and H2″ protons (1.7–3.0 ppm) is presented in Figure 6A. The sugar H1′ protons have been assigned by analysis of the NOESY data in Figure 4 so that it is straightforward to assign the sugar H2′ and H2″ protons to individual residues in Figure 6A. The cross-peak patterns differ for the H1′–H2′ and H1′–H2″ connectivities due to differences in coupling of the H2′ proton and H2″ proton with adjacent H1′ and H3′ protons. Previous studies have demonstrated that the H2′ proton resonates to high field of the H2″ proton except for a pattern reversal at the terminal 3′ residue in regular DNA helices (Hare et al., 1983; Weiss et al., 1984). We note that the H2′ protons are to high field of the H2″ protons in the O^{6}meG·C 12-mer except for a pattern reversal at the G2, O^{6}meG10, and 3′ terminal base G12 (Figure 6A). Thus, a comparison of these COSY connectivities in the G·C 12-mer (Hare et al., 1983) and the O^{6}meG·C 12-mer (Figure 6A) shows a reversal in H2′ and H2″ patterns for the purine residues at the modified C3·O^{6}meG10 base pair and G2·C11 base pair adjacent to it. The sugar H2′ and H2″ chemical shifts in the O^{6}meG·C 12-mer at 25 °C are summarized in Table II.

H2′ to H3′ COSY Connectivities. The cross section between the sugar H2′ and H2″ (1.7–2.8 ppm) and sugar H3′ (4.5–5.2 ppm) protons in the magnitude COSY spectrum of the O^{6}meG·C 12-mer is presented in Figure 6B. The cross peak between the H2′ proton and H3′ proton shows a distinct shape, and the H3′ protons can be assigned from the known H2′ assignments (Table II). We do not detect cross peaks between the H2″ and H3′ protons except for the 3′-terminal G12 residue, indicative of a small coupling constant between these protons for residues 1–11 in the O^{6}meG·C 12-mer duplex.

H3′ to H4′ COSY Connectivities. The cross section between the sugar H3′ (4.6–5.1 ppm) and the sugar H4′ (4.0–4.5 ppm)

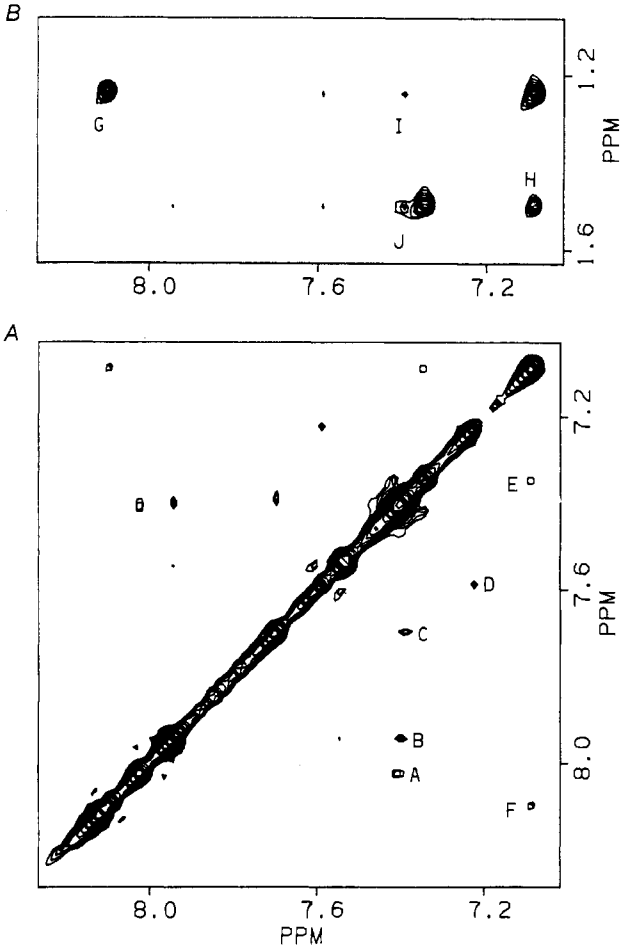

FIGURE 5: Expanded contour plot of the phase-sensitive NOESY spectrum (mixing time 250 ms) of the O^{6}meG·C 12-mer at 25 °C. (A) The distance connectivities are established amongst the base protons located between 7.0 and 8.2 ppm. The cross peaks A–F are assigned and discussed in the text. (B) The distance connectivities are established between the base protons (7.0–8.2 ppm) and the thymidine CH_3 protons (1.2–1.6 ppm). The cross peaks G–J are assigned and discussed in the text.

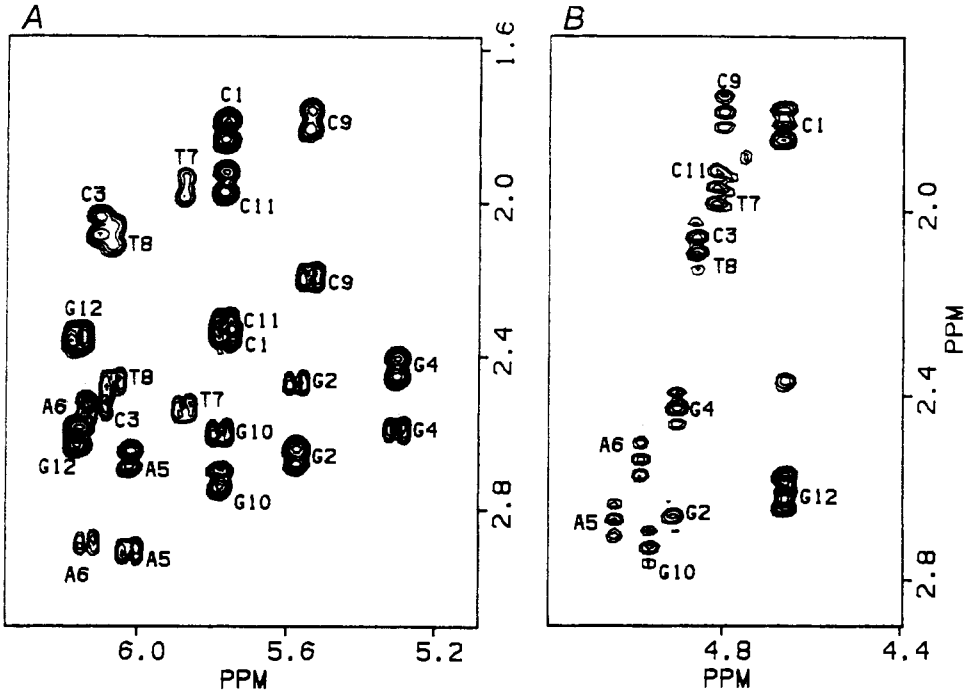

FIGURE 6: Expanded contour plot of the magnitude COSY spectrum of the O^{6}meG·C 12-mer at 25 °C, establishing connectivities (A) between the sugar H1′ protons (5.2–6.4 ppm) and the sugar H2′ and H2″ protons (1.7–3.0 ppm) and (B) between the sugar H2′ protons (1.7–2.8 ppm) and sugar H3′ protons (4.5–5.2 ppm).

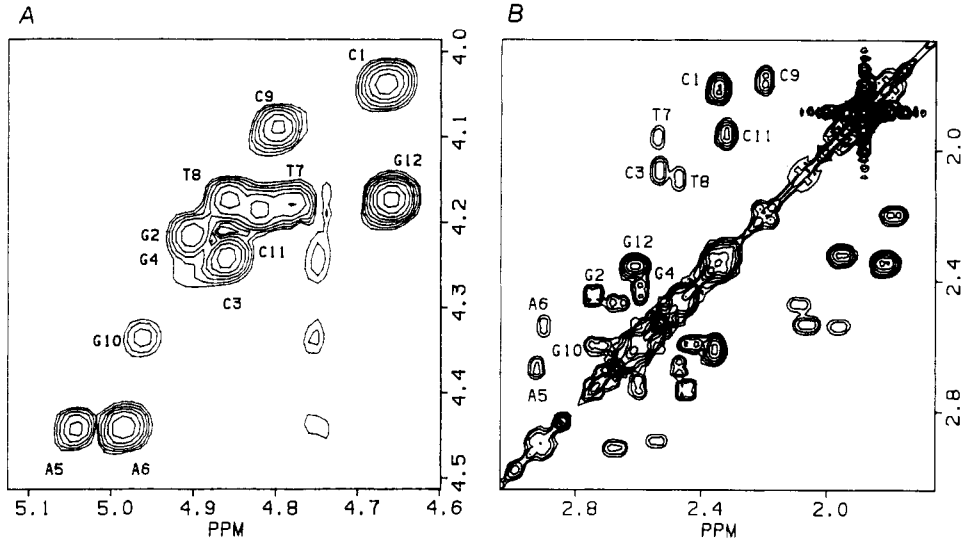

FIGURE 7: Expanded contour plot of the magnitude COSY spectrum of the O^{6}meG·C 12-mer at 25 °C, establishing coupling connectivities (A) between the sugar H3′ protons (4.6–5.1 ppm) and the H4′ protons (4.0–4.5 ppm) and (B) between the H2′ and H2″ protons in the spectral range 1.9–3.1 ppm.

protons in the magnitude COSY spectrum of the O^{6}meG·C 12-mer is presented in Figure 7A. The H4′ assignments readily follow from known H3′ assignments and are listed in Table II. We note that the O^{6}meG10 cross peak is weaker than the other resolved cross peaks in this spectral region (Figure 7A).

H2′ to H2″ COSY Connectivities. All 12 residues give resolved cross peaks between the H2′ and H2″ protons in the O^{6}meG·C 12-mer COSY spectrum spanning the symmetrical region 1.7–3.0 ppm (Figure 7B). The H2′ and H2″ assignments denoted in Figure 12 are consistent with those listed in Table II on the basis of the H1′ to H2′ and H2″ connectivities determined from Figure 6A.

Thus, we have used the sugar H1′ assignments determined from the NOESY experiment to assign the H2′, H2″, H3′, and H4′ protons in the COSY spectra of the O^{6}meG·C 12-mer duplex. No attempt has been made to assign the partially resolved H5′ and H5″ protons in the dodecanucleotide duplex.

Base to H3′ and H4′ NOESY Connectivities. An expanded region of the NOESY contour plot relating the base protons (7.0–8.2 ppm) with the H3′ protons (4.6–5.1 ppm) and the H4′ protons (4.0–4.5 ppm) in the O^{6}meG·C 12-mer is presented in Figure 8A. Each purine H8 and pyrimidine H6 proton exhibits an NOE to its own sugar H3′ residue and to the H3′ of the 5′-flanking sugar residue so that it is possible to walk between adjacent bases on a given strand by stepping through the H3′ protons. We do note that the H8 of O^{6}meG10 exhibits a strong NOE to its own H3′ but a weak NOE to the H3′ of the 5′-flanking C9 residue (designated by an arrow in Figure 8A) in the O^{6}meG·C 12-mer NOESY spectrum.

The H4′ and H5′ and H5″ protons are superpositioned in the contour plot in Figure 8A. The H4′ assignments have been analyzed from the COSY spectrum analysis (Table II), and these assignments are depicted in Figure 8A.

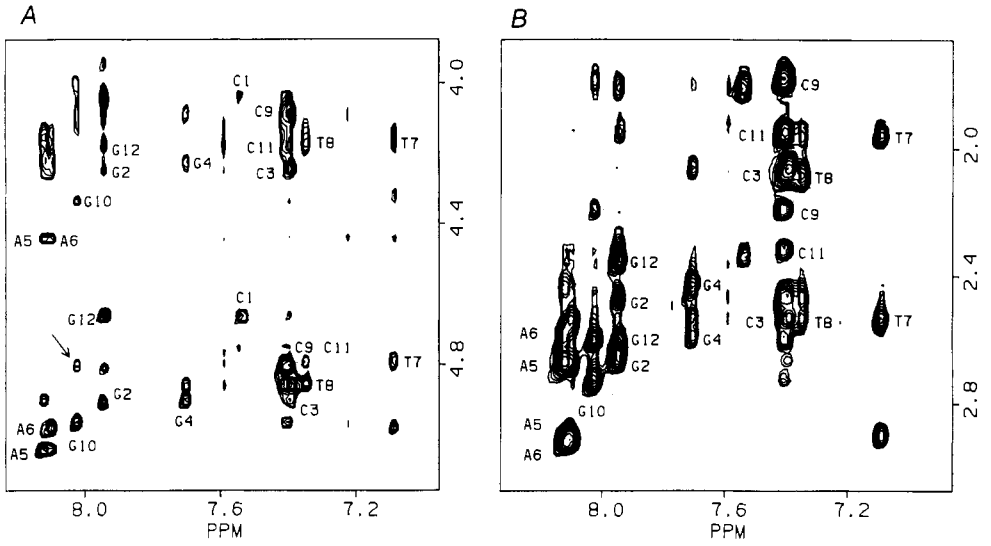

FIGURE 8: Expanded contour plot of the phase-sensitive NOESY spectrum (mixing time 250 ms) of the O⁶meG·C 12-mer at 25 °C, establishing distance connectivities (A) between the base protons (7.0–8.2 ppm) and the H3′ (4.6–5.1 ppm) and the H4′ (3.6–4.5 ppm) protons and (B) between the base protons (7.0–8.2 ppm) and the H2′ and H2″ protons (1.8–3.0 ppm).

Base to H2′ and H2″ NOESY Connectivities. An expanded region of the NOESY contour plot relating the base protons (7.0–8.2 ppm) with the H2′ and H2″ protons (1.7–3.0 ppm) in the O⁶meG·C 12-mer is depicted in Figure 8B. Cross peaks are observed between the pyrimidine H6 and purine H8 protons and the H2′ and H2″ protons of its own and 5′-connected sugars. The sugar H2′ and H2″ assignments are consistent with those depicted from the COSY spectrum analysis, and the assignments are depicted in Figure 8B.

NOESY Connectivities in Other Regions. The NOESY data presented above have focused on the cross peaks between the base protons and the sugar H1′, H2′, H2″, H3′, and H4′ protons in the O⁶meG·C 12-mer duplex. This analysis has also been extended to NOE cross peaks between various sets of sugar protons observed in Figure 3B. Thus, the H1′ protons exhibit NOEs to their own H2′, H2″, H3′, and H4′ protons but not those of their 5′- and 3′-flanking sugars (Figure 3B). These NOEs provide cross-checks for the O⁶meG·C 12-mer assignments listed in Table II.

O⁶meG Base Proton NOEs. We have taken a one-dimensional slice through the resolved H8 proton of O⁶meG10 (8.005 ppm) in the H1′ (5.3–5.9 ppm), H3′ (4.7–5.1 ppm), and H2′ and H2″ (1.6–2.9 ppm) spectral regions of the 250-ms NOESY spectrum of the O⁶meG·C 12-mer duplex. We observe larger NOEs to the sugar protons of its own O⁶meG10 sugar compared to those of the 5′-flanking C9 sugar. An NOE is also observed between the H8 of O⁶meG10 and the H5 of C11 in the purine(3′–5′)pyrimidine O⁶meG10–C11 step in the O⁶meG·C 12-mer duplex.

We can monitor NOEs between the CH_3 group of O⁶meG10 and adjacent base protons in the O⁶meG·C 12-mer duplex. We have taken a one-dimensional slice through the OCH_3 proton of O⁶meG10 (3.44 ppm) in the base (7.1–8.3 ppm) and sugar H1′ (5.2–6.4 ppm) spectral regions. We detect NOEs between the CH_3 of O⁶meG10 and the H5 of C9 and a weaker effect at the H6 of C9 in the C9–O⁶meG10 segment of the duplex.

Phosphodiester Backbone. The proton-decoupled phosphorus spectra of the G·C 12-mer duplex (Patel et al., 1982) and the O⁶meG·C 12-mer duplex at 7 °C (Figure 9) exhibit different spectral dispersions. The 11 phosphodiesters are dispersed over 0.7 ppm in the unmodified dodecanucleotide (Patel et al., 1982) and over 1.3 ppm in the O⁶meG·C-modified duplex at 7 °C (Figure 9). Three of the eleven phosphates in the O⁶meG·C 12-mer duplex resonate outside the 4.0–4.5 ppm spectral region (Figure 9), characteristic of phosphodiesters with an unperturbed O–P torsion angle. We have monitored the temperature dependence of the phosphorus spectrum of the O⁶meG·C 12-mer and note that the downfield-shifted phosphorus resonance broadens and coalesces with the main envelope on raising the temperature (Figure 9). The spectral dispersion decreases to 0.25 ppm in the O⁶meG·C 12-mer in the strand state at 55 °C (Figure 9).

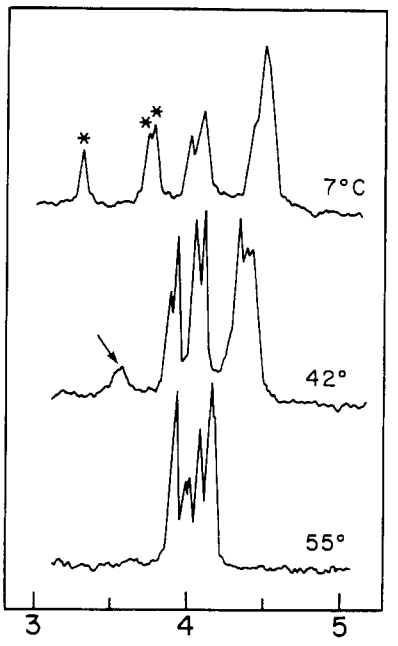

FIGURE 9: Proton noise-decoupled 81-MHz phosphorus NMR spectra of the O⁶meG·C 12-mer duplex in 0.1 M NaCl, 10 mM phosphate, 1 mM EDTA, and D_2O, pH 8.05, as a function of temperature between 7 and 55 °C. Chemical shifts are corrected for the temperature dependence of the internal standard trimethyl phosphate.

DISCUSSION

Imino Proton Shifts and Widths. The C3·O⁶meG10 interaction lacks an imino proton, and therefore, it is not surprising that only five imino proton resonances are detected between 12 and 14 ppm in the O⁶meG·C spectrum in 0.1 M NaCl, 10 mM phosphate, and H_2O, neutral pH at low temperature (Figure 2A). These imino protons have been assigned from one-dimensional NOEs that link protons within a base

pair (H3 of T and H2 of A, H1 of G and H4 of C) and between adjacent base pairs (Figure 1), and their chemical shifts are summarized in Table I. These results demonstrate that the base pairs G2·C11 and G4·C9 on either side of the modification site in the O^{6}meG·C 12-mer are stable at low temperature in aqueous solution.

We do not detect NOEs between the imino protons of G2·C11 and G4·C9 in the O^{6}meG·C 12-mer at 10 °C (Figure 1C,D). This rules out a model in which the C3 and O^{6}meG10 bases loop out of the helix and the flanking G2·C11 and G4·C9 base pairs stack on each other. Rather, the data document stacking of C3 and O^{6}meG10 into the helix, thus providing a spacer between the flanking G2·C11 and G4·C9 base pairs in the O^{6}meG·C 12-mer duplex.

We note that the imino proton of G4·C9 (12.34 ppm) in the O^{6}meG·C 12-mer duplex is upfield from its corresponding value (12.64 ppm) in the G·C 12-mer duplex (Patel et al., 1982c) while the other imino protons exhibit similar chemical shifts in the two duplexes at −5 °C. This supports a change in stacking pattern between C3·O^{6}meG10 and G4·C9 base pairs in the O^{6}meG·C 12-mer duplex compared to the stacking pattern between C3·G10 and G4·C9 base pairs in the G·C 12-mer duplex.

The sequential broadening of the imino protons of C1·G12 followed by those of G2·C11 with increasing temperature (Figure 2A) is consistent with fraying at the ends of the O^{6}meG·C 12-mer duplex. The imino protons of G4·C9, A5·T8, and A6·T7 broaden out simultaneously above 45 °C in the O^{6}meG·C 12-mer duplex compared to similar behavior above 60 °C in the G·C 12-mer duplex (Patel et al., 1982c). Thus, replacement of two C3·G10 base pairs by two C3·O^{6}meG10 interactions results in a destabilization of the duplex similar to what was observed in the optical melting studies (Gaffney et al., 1984).

The imino protons of A5·T8 and A6·T7 exhibit the largest temperature dependence while the imino protons of G4·C9 exhibit the smallest temperature dependence in the O^{6}meG·C 12-mer (Figure 2B) similar to what was observed previously in the G·C 12-mer duplex (Patel et al., 1982c).

Nonexchangeable Proton Shifts. We have assigned the nonexchangeable base and sugar protons in the O^{6}meG·C 12-mer in 0.1 M NaCl and D_2O, 25 °C, from an analysis of the magnitude COSY (Figure 3A) and the 250-ms mixing time phase-sensitive NOESY (Figure 3B) two-dimensional spectra. These assignments are listed in Table II, and the O^{6}meG·C 12-mer chemical shifts are compared with those reported for the G·C 12-mer by one-dimensional (Patel et al., 1982c) and two-dimensional (Hare et al., 1983) methods. The base and sugar proton chemical shifts are similar for the terminal C1·G12 and central A5·T8 and A6·T7 base pairs but differ between the G·C 12-mer and O^{6}meG·C 12-mer at the G2·C11, C3·O^{6}meG10, and G4·C9 base pairs.

Base proton chemical shift differences are observed at the H8 proton of G4 (−0.15 ppm) and G10 (0.12 ppm) and H6 proton of C3 (0.14 ppm) on proceeding from the G·C 12-mer to the O^{6}meG·C 12-mer duplexes. Sugar proton chemical shift differences of 0.1–0.3 ppm are observed at the H1′, H2′, and H2″ protons of G2, G4, and C9 with the most pronounced difference at the H1′ (0.55 ppm), H2′ (0.26 ppm), and H2″ (0.33 ppm) of C3 on proceeding from the G·C 12-mer to the O^{6}meG·C 12-mer duplex. These chemical shift differences are indicative of changes in base pair overlaps and/or torsion angles at (C3·O^{6}meG10) and adjacent to (G2·C11 and G4·C9) the modification site. It is not possible to translate sugar chemical shift changes in conformational terms at this time.

Right-Handed Duplex. Many of the NOEs detected in the NOESY spectrum of the O^{6}meG·C 12-mer duplex exhibit directionality indicative of the handedness of the duplex. For right-handed helices, one observes the following patterns of directional NOEs: (a) The purine H8 and pyrimidine H6 protons exhibit NOEs to the sugar H1′, H2′, H2″, and H3′ protons of their own and 5′-linked sugars but not their 3′-linked sugars. (b) The pyrimidine H5 and CH_3 protons exhibits NOEs to the H1′, H2′, H2″, and H3′ protons of their 5′-linked sugars only. (c) The purine H8 and pyrimidine H5 and CH_3 protons exhibit NOEs in the purine(3′–5′)pyrimidine step but not the pyrimidine(3′–5′)purine step. (d) The adenosine H2 proton in the minor groove exhibits NOEs to the sugar H1′ protons of its own sugar, the 3′-linked sugar on the same strand, and the sugar in the opposite direction on the partner strand. The NOEs detected in the O^{6}meG·C 12-mer duplex meet the above criteria, and the helix must be right-handed in solution.

Glycosidic Torsion Angles. Previous studies have shown that the syn conformation about the glycosidic bond can be readily identified on the basis of a NOE between the base (purine H8 and pyrimidine H6) and its own sugar H1′ proton (interproton distance ~2.4 Å), which has a cross-peak intensity comparable to the NOE between the cytidine H5 and H6 protons (interproton distance ~2.4 Å) (Patel et al., 1983). By contrast, the base to H1′ NOE (interproton distance ~3.7 Å) is much weaker than the cytidine H5–H6 NOE for an anti conformation about the glycosidic bond. We note that all the base to H1′ cross peaks are much weaker in intensity than the cytidine H5–H6 cross peaks (designated by asterisks) for the O^{6}meG·C 12-mer duplex at 25 °C (Figure 4). This demonstrates that the glycosidic torsion angles are anti at the C3·O^{6}meG10 modification site as they are at all the residues in the O^{6}meG·C 12-mer duplex.

C3·O^{6}meG10 Modification Site. We stated above that the H8 of purines exhibits NOEs to the H1′, H2′, H2″, and H3′ of its own sugar and its 5′-linked sugar, which are of comparable magnitude for right-handed helices in solution. We do note, however, that for O^{6}meG10 the NOE is larger to its own compared to the 5′-linked sugar residue in the O^{6}meG·C 12-mer duplex (Figures 4 and 8). This is clearly observed in the one-dimensional slice through the 8.005 ppm H8 proton of O^{6}meG10 covering the H1′, H3′, H2′, and H2″ spectral regions. Thus, the conformation of the O^{6}meG10 base relative to its own O^{6}meG10 sugar and the C9 flanking sugar in the C9–O^{6}meG10 step in the O^{6}meG·C 12-mer duplex differs from that observed for a regular right-handed duplex.

We detect an NOE between the H8 proton of O^{6}meG10 and the H5 of C11 in the O^{6}meG10–C11 purine(3′–5′)pyrimidine step (peak A, Figure 4) in the O^{6}meG·C 12-mer duplex. This is a characteristic pattern for regular right-handed DNA, and hence, the overlap between O^{6}meG10 and C11 adopts the normal pattern in the O^{6}meG·C 12-mer duplex.

We have monitored the NOEs between the OCH_3 of O^{6}meG10 and nearby protons in the NOESY spectrum of the O^{6}meG·C 12-mer duplex at 25 °C (Figure 3B). The strongest NOE is to the H5 proton of adjacent C9, and a weaker NOE is observed at the H6 proton of the same base in a one-dimensional slice through the CH_3 of O^{6}meG10. Thus, the OCH_3 of O^{6}meG10 remains in the major groove and overlaps with the H5 of C9 also located in the major groove of the O^{6}meG·C 12-mer duplex.

The 3.44 ppm chemical shift of the O^{6}meG residue in the O^{6}meG·C 12-mer duplex at 25 °C is upfield from its strand value of ~3.95 ppm. This demonstrates that the O^{6}meG

Chart II

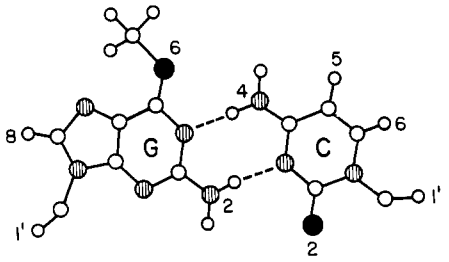

group stacks with adjacent G2·C11 and G4·C9 base pairs in the duplex state.

We detect phosphorus resonances at 3.26, 3.69, and 3.72 ppm in the O^{6}meG·C 12-mer duplex at 7 °C, which resonate outside the 4.0–4.5 ppm spectral region for regular right-handed duplexes (Figure 9). This suggests that three phosphodiesters adopt altered O–P torsion angles, though we are unable to assign them in the O^{6}meG·C 12-mer duplex at this time. Potential candidates are the phosphates flanking the O^{6}meG10 and C3 bases at the modification site. These shifted resonances coalesce into the main spectral dispersion on raising the temperature of the O^{6}meG·C 12-mer to 55 °C, indicative of conversion to strand states.

We have no direct evidence to define the potential pairing of the C3 and O^{6}meG10 bases at the modification site in the O^{6}meG·C 12-mer duplex. It is clear, however, that proceeding from C3·G10 in the G·C 12-mer to C3·O^{6}meG10 in the O^{6}meG·C 12-mer does not result in a large perturbation since we can still monitor the base to H1′ NOEs from C1 to G12 (Figure 4) and the base to base NOEs in the O^{6}meG10–C11 step (peak A, Figure 4). A proposed pairing scheme for the C3·O^{6}meG10 interaction is presented in Chart II in which the O^{6}meG10 base slides somewhat toward the major groove while the C3 base slides toward the minor groove, resulting in two amino-ring nitrogen hydrogen bonds. We tentatively propose this pairing scheme for the C3·O^{6}meG10 interaction as a working model for designing future experiments to test its validity.

Chemical Shift Comparison in the G·C 12-mer and O^{6}meG·C 12-mer Duplexes. The base protons of G2·C11 and G4·C9 flanking the modification site exhibit similar chemical shifts except for a 0.30 ppm upfield shift for the imino proton of G4 and an 0.15 ppm upfield shift for the H8 of G4 on proceeding from the G·C 12-mer to the O^{6}meG·C 12-mer duplex (Table III). This suggests that G4·C9 overlaps differently with C3·G10 in the G·C 12-mer compared to C3·O^{6}meG10 in the O^{6}meG·C 12-mer duplex. Alternately, the hydrogen-bond geometry and/or strength at the G4·C9 base pair may differ in the G·C 12-mer and O^{6}meG·C 12-mer duplexes.

We also observe chemical shift differences for the sugar H1′ protons in the G·C 12-mer and O^{6}meG·C 12-mer duplexes. The largest changes are a 0.29 ppm upfield shift for the H1′ proton of G2 and a 0.55 ppm downfield shift for the H1′ of C3 on proceeding from the G·C 12-mer to the O^{6}meG·C 12-mer duplexes (Table III). The sugar H1′ protons are sensitive to glycosidic torsion angle changes, and the results suggest that there are variations within the anti glycosidic torsion angle range at C3 and G2 between the two duplexes.

The phosphorus chemical shift dispersion increases from 0.6 ppm in the G·C 12-mer to 1.2 ppm in the O^{6}meG·C 12-mer duplex at 7 °C. We observe three shifted phosphorus resonances in the modified duplex, suggestive of O–P torsion angle changes for at least three phosphates between the G·C 12-mer and O^{6}meG·C 12-mer duplexes.

Table III: Comparison of the Base Proton Chemical Shifts in the G·C 12-mer and O^{6}meG·C 12-mer Duplexes in 0.1 M Salt at 25 °C

		chemical shifts (ppm)	
base pair	proton	G·C 12-mer[a]	O^{6}meG·C 12-mer
G2·C11	G H1	13.04	13.04
	G H8	7.92	7.93
	C H6	7.30	7.38
	C H5	5.41	5.39
	G H1′	*5.84*	*5.55*
	C H1′	5.73	5.75
G4·C9	G H1	*12.64*	*12.34*
	G H8	7.83	7.68
	C H6	7.44	7.38
	C H5	5.61	5.58
	G H1′	5.42	5.29
	C H1′	5.67	5.52
C3·*G10[b]	*G H8	7.89	8.01
	C H6	7.24	7.38
	C H5	5.35	5.39
	*G H1′	5.82	5.77
	C H1′	*5.55*	*6.10*

[a] Data taken from Patel et al. (1982) and Hare et al. (1983). [b] *G-10 signifies G in the G·C 12-mer and O^{6}meG in the O^{6}meG·C 12-mer.

The above qualitative conclusions based on chemical shift variations suggest potential sites of conformational differences between the G·C 12-mer and the O^{6}meG·C 12-mer duplexes.

ACKNOWLEDGMENTS

The two-dimensional NMR spectra were recorded at Northeast Regional NMR Facility WM 500 at Yale University, which is supported by National Science Foundation Grant CHE-7916210. We thank Dr. Dennis Hare for providing access to his two-dimensional NMR processing software and guidance in its usage.

Registry No. O^{6}meG·C 12-mer, 92984-22-0; O^{6}meG, 76567-63-0; C, 71-30-7.

REFERENCES

Cairns, J. (1981) *Nature (London) 289*, 353–357.
Fazakerley, G. V., van der Marel, G. A., van Boom, J. H., & Guschlbauer, W. (1984) *Nucleic Acids Res. 12*, 8269–8279.
Feigon, J., Leupin, W., Denny, W. A., & Kearns, D. R. (1983) *Biochemistry 22*, 5943–5951.
Fowler, K. W., Buchi, G., & Essigmann, J. M. (1982) *J. Am. Chem. Soc 104*, 1050–1054.
Gaffney, B. L., Marky, L. A., & Jones, R. A. (1984) *Biochemistry 23*, 5686–5691.
Green, C. L., Loechler, E. L., Fowler, K. W., & Essigmann, J. M. (1984) *Proc. Natl. Acad. Sci. U.S.A. 81*, 13–17.
Haasnoot, C. A. G., & Hilbers, C. W. (1983) *Biopolymers 22*, 1259–1266.
Hare, D. R., Wemmer, D. E., Chou, S. H., Drobny, G., & Reid, B. R. (1983) *J. Mol. Biol. 171*, 319–336.
Kearns, D. R. (1984) *CRC Crit. Rev. Biochem. 15*, 237–290.
Kuzmich, S., Marky, L. A., & Jones, R. A. (1983) *Nucleic Acids Res. 11*, 3393–3404.
Loechler, E. L., Green, C. L., & Essigman, J. M. (1984) *Proc. Natl. Acad. Sci. U.S.A. 81*, 6271–6275.
Loveless, A. (1969) *Nature (London) 223*, 206–207.
McConnel, B. (1984) *J. Biomol. Struct. Dyn. 1*, 1402–1421.
Patel, D. J. (1976) *Biopolymers 15*, 533–558.
Patel, D. J., & Hilbers, C. W. (1975) *Biochemistry 14*, 2651–2656.
Patel, D. J., Pardi, A., & Itakura, K. (1982a) *Science (Washington, D.C.) 216*, 581–590.
Patel, D. J., Kozlowski, S. A., Rice, J. A., Marky, L. A., Breslauer, K. J., Broka, C., & Itakura, K. (1982b) in *Topics in Nucleic Acid Structure* (Neidle, S., Ed.) Vol. 2, pp

81–136, Macmillan, New York.
Patel, D. J., Kozlowski, S. A., Marky, L. A., Broka, C., Rice, J. A., Itakura, K., & Breslauer, K. J. (1982c) *Biochemistry 21*, 428–436.
Patel, D. J., Kozlowski, S. A., Nordheim, A., & Rich, A. (1983) *Proc. Natl. Acad. Sci. U.S.A. 79*, 1413–1417.
Patel, D. J., Shapiro, L., Kozlowski, S. A., Gaffney, B. L., & Jones, R. A. (1986) *Biochemistry* (following paper in this issue).
Redfield, A. G., Kunz, S. D., & Ralph, E. K. (1975) *J. Magn. Reson. 19*, 114–117.
Scheek, R. M., Boelens, R., Russo, N., van Boom, J. H., & Kaptein, R. (1984) *Biochemistry 23*, 1371–1376.
Singer, B. (1979) *JNCI, J. Natl. Cancer Inst. 62*, 1329–1339.
Singer, B., & Grunberger, D. (1983) in *Molecular Biology of Mutagens and Carcinogens*, Plenum, New York.
States, D. J., Haberkorn, R. A., & Ruben, D. J. (1982) *J. Magn. Reson. 48*, 286–292.
Weiss, M., Patel, D. J., Sauer, R. T., & Karplus, M. (1984a) *Proc. Natl. Acad. Sci. U.S.A. 81*, 130–134.
Weiss, M., Patel, D. J., Sauer, R. T., & Karplus, M. (1984b) *Nucleic Acids Res. 12*, 4035–4047.

Structural Studies of the O^{6}meG·T Interaction in the d(C-G-T-G-A-A-T-T-C-O^{6}meG-C-G) Duplex†

Dinshaw J. Patel* and Lawrence Shapiro
Department of Biochemistry and Molecular Biophysics, College of Physicians and Surgeons, Columbia University, New York, New York 10032
Sharon A. Kozlowski
Polymer Chemistry Department, AT&T Bell Laboratories, Murray Hill, New Jersey 07994
Barbara L. Gaffney and Roger A. Jones
Department of Chemistry, Rutgers, The State University of New Jersey, New Brunswick, New Jersey 08903
Received July 16, 1985

ABSTRACT: High-resolution proton and phosphorus NMR studies are reported on the self-complementary d(C_1-G_2-T_3-G_4-A_5-A_6-T_7-T_8-C_9-O^{6}meG$_{10}$-C_{11}-G_{12}) duplex (henceforth called O^{6}meG·T 12-mer), which contains T3·O^{6}meG10 interactions in the interior of the helix. The imino proton of T3 is observed at 9.0 ppm, exhibits a temperature-independent chemical shift in the premelting transition range, and broadens out at the same temperature as the imino proton of the adjacent G2·C11 toward the end of the helix at pH 6.8. We observed inter base pair nuclear Overhauser effects (NOEs) between the base protons at the T3·O^{6}meG10 modification site and the protons of flanking G2·C11 and G4·C9 base pairs, indicative of the stacking of the T3 and O^{6}meG10 bases into the helix. Two-dimensional correlated (COSY) and nuclear Overhauser effect (NOESY) studies have permitted assignment of the base and sugar H1′, H2′, and H2″ nonexchangeable protons in the O^{6}meG·T 12-mer duplex. The observed NOEs demonstrate an anti conformation about all the glycosidic bonds, and their directionality supports formation of a right-handed helix in solution. The observed NOEs between the T3·O^{6}meG10 interaction and the adjacent G2·C11 and G4·C9 base pairs at the modification site exhibit small departures from patterns for a regular helix in the O^{6}meG·T 12-mer duplex. The phosphorus resonances exhibit a 0.5 ppm spectral dispersion indicative of an unperturbed phosphodiester backbone for the O^{6}meG·T 12-mer duplex. We propose a model for pairing of T3 and O^{6}meG10 at the modification site in the O^{6}meG·T 12-mer duplex. This study compares the NMR parameters of the O^{6}meG·T 12-mer duplex with those of the G·T 12-mer duplex, which contains a T3·G10 mismatch at the same site in the helix.

The mutagenic and carcinogenic lesion resulting from the O^6-alkylation of guanosine (O^{6}meG) has been the focus of extensive biological studies to elucidate the consequences of this simple covalent modification of DNA. These studies include the base pairing properties of O^{6}meG in template DNA during in vitro replication (Snow et al., 1984) and in vivo mutagenesis studies following site-specific incorporation of O^{6}meG in viral genomes (Green et al., 1984; Loechler et al., 1984). The latter studies demonstrated that O^{6}meG induced exclusively G → A transitions indicative of O^{6}meG·T pairing in the viral genome.

Chart I

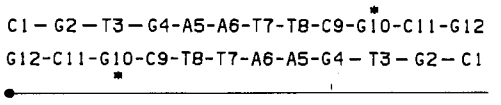

It has also been shown that the conversion of normal genes to oncogenes can result from G → A transition errors (Santos et al., 1983) and also from G → T transversion errors at a single G residue in the *ras* system (Tabin et al., 1982; Reddy

† This research was supported by National Institutes of Health Grant 1R01 GM34504 to D.J.P. and by American Cancer Society Grant CH-248 and National Institutes of Health Grant GM31483 to R.A.J. L.S. was supported by Biochemical Research Support Grant SO7RR05359-23.

0006-2960/86/0425-1036$01.50/0